Neuropathology and Applied Neurobiology

Early changes in extracellular matrix in Alzheimer's disease

Journal:	*Neuropathology and Applied Neurobiology*
Manuscript ID	NAN-2015-0082.R2
Manuscript Type:	Original Article
Date Submitted by the Author:	n/a
Complete List of Authors:	Lepelletier, Francois-Xavier; University of Manchester, Wolfson Molecular Imaging Centre; University of Manchester, Faculty of Medical and Human Sciences, Institute of Brain, Behaviour and Mental Health Mann, David; University of Manchester, Faculty of Medical and Human Sciences, Institute of Brain, Behaviour and Mental Health Robinson, Andrew; University of Manchester, Institute of Brain, Behaviour and Mental Health; Salford Royal NHS Foundation Trust, Department of Clinical & Cognitive Neurosciences Pinteaux, Emmanuel; University of Manchester, Faculty of Life Sciences Boutin, Herve; University of Manchester, Wolfson Molecular Imaging Centre; University of Manchester, Faculty of Medical and Human Sciences
Keywords:	Alzheimer's disease, extracellular matrix, basement membrane, collagen IV, perlecan, fibronectin, hPECAM, von Willebrand factor

Early changes in extracellular matrix in Alzheimer's disease

François-Xavier Lepelletier[a,b], David M A Mann[b,c], Andrew C Robinson[b,c], Emmanuel Pinteaux[d], Hervé Boutin[a,e]

[a] Wolfson Molecular Imaging Centre, University of Manchester, 27 Palatine road, Manchester M20 3LJ, United Kingdom

[b] Faculty of Medical and Human Sciences, Institute of Brain, Behaviour and Mental Health, University of Manchester, Manchester, United Kingdom

[c] Salford Royal NHS Foundation Trust, Department of Clinical & Cognitive Neurosciences, Salford Royal-Room A304, Clinical Sciences Building, Salford M6 8FJ, United Kingdom

[d] Faculty of Life Sciences, University of Manchester, AV Hill Building 2.025B, Oxford road, Manchester M13 9PT, United Kingdom

[e] Faculty of Medical and Human Sciences, Institute of Population Health, University of Manchester, Manchester, United Kingdom

Corresponding author:

Hervé Boutin, Wolfson Molecular Imaging Centre, University of Manchester, 27 Palatine Road, Manchester, M20 3LJ, UK.
e-mail: herve.boutin@manchester.ac.uk
phone: +44 161 275 0078

Keywords:

Alzheimer's disease; extracellular matrix; basement membrane; collagen IV; perlecan; fibronectin; hPECAM; vWF.

Number of words: 3985

Number of figures: 7 + 1 supplementary figure

Number of tables: 2

Abstract

AIMS: Although changes in extracellular matrix (ECM) scaffold have been reported previously in AD compared to normal ageing, it is not known how alterations in the numerous components of the perivascular ECM might occur at different stages of AD. This study therefore investigates potential changes in basement membrane-associated ECM molecules in relation to increasing Braak stages.

METHODS: Thirty patients were divided into three groups (control subject, subclinical AD and AD patients). ECM levels of collagen IV, perlecan and fibronectin as well as human platelet endothelial cell adhesion molecule (hPECAM) were quantified by immunohistochemistry. Von Willebrand factor staining was measured to assess vessel density. Expression levels were correlated with the presence of amyloid plaques.

RESULTS: Collagen IV, perlecan and fibronectin expression was increased in subclinical AD and AD patients when compared to controls, in frontal and temporal cortex, whilst no further increase was detected between subclinical AD and AD. These changes were not associated with an increase in vessel density, which was instead decreased in the temporal cortex of AD patients. In contrast, hPECAM levels remained unchanged. Finally, we found similar pattern in levels of amyloid deposition between the different Braak stages and showed that changes in ECM components correlated with amyloid deposition.

CONCLUSION: Present data support the hypothesis that significant ECM changes occur during the early stages of AD. ECM changes affecting brain microvascular functions could therefore drive disease progression and provide potential new early investigational biomarkers in AD.

Introduction

Alzheimer's disease (AD) is a chronic and progressive neurodegenerative disease, and is the most common form of dementia amongst the elderly population. It is characterized by memory loss and cognitive decline. Among the hallmarks of AD, the most well characterized are the presence of numerous extracellular (senile) plaques (SP) and neurofibrillary tangles (NFT) in neocortical and some subcortical brain regions [1]. The extracellular plaques consist of aggregates of amyloid β protein (Aβ), which is a breakdown product of amyloid β precursor protein (APP) when cleaved by β- and γ-secretases. NFT result from an aggregation of abnormally phosphorylated microtubule-associated tau proteins. In the cerebral cortex, amyloid deposits and tau aggregation show a characteristic distribution pattern following a predictable sequence over the course of the disease [2, 3]. It has previously been described in animal models that extracellular matrix (ECM) components can influence β amyloid fibrillogenesis, and thereby may contribute to AD progression [4, 5]. Moreover, Aβ seems to interact with a variety of proteoglycans and fibrous proteins [6-11]. Aβ deposition, as well as neurodegeneration, is highly damaging to the integrity of the pre-existing ECM, resulting in a deterioration of physico-chemical properties, such as diffusion parameters of the extracellular micromilieu [12, 13].

The ECM constitutes the essential physical scaffolding for cells, and acts as a biomechanical and biochemical support required for tissue rearrangement, differentiation and homeostasis [14]. The functional attributes of the ECM in the adult central nervous system (CNS) arise directly from their molecular composition, which is localized into three principal compartments: the neural interstitial matrix, the perineuronal nets and the basement membrane. The latter is a sheet-like layer that serves as a boundary between CNS parenchymal tissue and endothelial cells and is predominantly made up of collagen, fibronectin and proteoglycans such as perlecan [15]. Collagen type IV is the most abundant fibrous protein within the interstitial ECM. Collagen IV is essential for regulating cell adhesion and directing tissue development through its role in chemotaxis and cell migration, while also providing strength to the ECM [16]. Perlecan interacts with several other components of the ECM, and is an essential component of the vascular ECM involved in maintenance of the endothelial barrier function [17]. Fibronectin is directly involved in mediating cell attachment and function and, as such, in directing the (re-)organization of the interstitial ECM [14].

Another component of the basement membrane, the human platelet endothelial cell adhesion molecule (hPECAM), has a higher level of expression at the endothelial cell junction, is involved in cell adhesion, and acts as a signalling molecule [18] through interactions with the ECM [19].

ECM changes have been reported in both normal ageing and in AD, and this remodelling could mediate cell proliferation, differentiation and apoptosis [20, 21]. The functional consequences of this remodelling may be dependent on the local specific organization of the ECM as established in animal models [22-25]. Any, or all, of these key ECM components might be affected during AD pathogenesis, though previous reports have described contradictory changes in ECM components in AD. For example, some reports found an increase in collagen IV in cerebral microvessels in AD and Parkinson's disease [26-28], while other reports have shown a decrease [29] or no change in intensity of staining [30] in cortical vessels in AD. As regards proteoglycans such as perlecan, these ECM components have been shown to be present in both amyloid plaques and NFT. They are thought to contribute to disease pathogenesis by accelerating the formation of Aβ through preventing proteolytic degradation [10, 31]. Total uronic acids, as basic components of the proteoglycan perlecan, have been reported to be increased in cerebral microvessels in AD [26]. Conversely, no significant difference was seen in perlecan mRNA levels in the hippocampus in AD when compared to age-matched controls, indicating that perlecan expression may remain stable in AD [32]. In the case of fibronectin, it has been previously reported that high molecular fibronectin forms appear more frequently and at higher amounts in plasma in AD than in age-matched controls [33], and that levels of plasma fibronectin are higher in AD than in healthy controls and individuals with mild cognitive impairment [34]. On the other hand, unchanged plasma fibronectin concentrations have also been described in AD [35].

To date, no studies have compared the expression of different ECM components within the same groups of control and AD patients, or have investigated changes in ECM components in relation to disease progression, as classified by Braak staging [2]. Therefore, the aim of the present study was to identify changes in ECM in healthy control subjects with low (Braak ≤2), intermediate (Braak >2 & ≤4) and high Braak stages (Braak >4). We have used immunohistochemistry to look for changes in three major ECM components - collagen IV, perlecan, fibronectin - as well as a

cell adhesion and signalling molecule, hPECAM - in the cerebral cortical grey matter of these individuals. We also assessed the severity of Aβ plaque formation to test for potential correlations between plaque load and potential changes in collagen IV, perlecan, fibronectin and hPECAM. Finally, we assessed capillary density by immunostaining for the von Willebrand factor (vWF), a multimeric glycoprotein present in blood plasma and produced largely in endothelium and megakaryocytes, which has been widely used to demonstrate vessels in tissue [36].

Materials and methods

Patients

Thirty cases (9 men and 21 women) were investigated, and *post-mortem* brain tissues were obtained from the Manchester Brain Bank through appropriate consenting procedures for the collection and use of human brain tissues (Manchester Brain Bank Generic Tissue Bank Ethical Approval number 09/H0906/52). Pathological diagnoses were made by an experienced neuropathologist (DM) as previously described [37, 38], and in accordance with recent National Institute on Ageing - Alzheimer's Association guidelines for the neuropathological assessment of AD [39]. By such classification, only cases with Braak stages 5 and 6 were classed as definite AD. Cases with Braak Stages >2 & ≤4 were not diagnosed as definite AD, but these could be considered as cases of possible (incipient) AD, thereby representing cases with early changes of AD. Amyloid plaque load *per se* was not employed for classification of AD, although it is acknowledged that neuritic plaque scores do form the basis of CERAD classification. Clearly, in terms of amyloid plaques alone, there was overlap in amyloid load between cases at Braak stage >2 & ≤4 and those at Braak stages 5 and 6. Subjects were therefore split in three groups based on their Braak stages [2]: controls (Braak ≤2, 12 subjects), subclinical AD (Braak >2 & ≤4, 10 subjects) and AD (Braak >4, 8 subjects). Details of each case are described in Table 1. Hence, brains in the first group were considered as a (normal) control group (Braak ≤2). These were obtained from aged patients with no history of neurological disease and no pathological evidence of AD or other degenerative brain disease. The second group (subclinical AD, Braak >2 & ≤4) consisted of patients with mild to moderate AD-type pathology, whilst the last group (moderate to severe AD, Braak >4) all showed abundant

plaques and tangles throughout all cortical regions and met pathological criteria for established AD [39, 40]. The mean age at death was not significantly different between the control group (82.0±11.4; range 54-95 years) and both AD groups (89.0±4.5 [range 82-97 years] and 77.9±9.0 years [range 62-91 years] for subclinical AD and AD groups, respectively), although subclinical AD and AD groups were significantly different ($P<0.05$, Kruskal-Wallis test with Dunn's *post-hoc* analysis). The average *post-mortem* delay was also similar for all groups (38.5±14.8; 32.7±12.8 and 45.1±16.5 hours for controls, subclinical AD and AD groups, respectively), and was less than 72 hours in all cases.

Immunohistochemistry

Fluorescent labelling

Sections of superior frontal gyrus (Brodmann areas 8/9) and inferior temporal gyrus (Brodmann areas 21/22) were cut at 20 µm thickness from fresh frozen tissue blocks and mounted on to glass slides (SuperFrost Plus®, Thermo Fisher Scientific Inc., MA, USA). For all the following experiments described below, buffer refers to 0.1M phosphate buffer (pH 7.4) (Sigma, St. Louis, MO, USA). Sections were first fixed by immersion in 4% paraformaldehyde (Sigma) buffer for 10 minutes, and then incubated in sodium borohydride buffer (1 mg/ml, Sigma) for 8 minutes to prevent auto-fluorescence. They were then incubated for 2 hours at room temperature in blocking buffer containing 3% donkey serum and 0.1% triton X-100. Tissue sections were thereafter incubated overnight at 4°C with primary antibody (see Table 2) in 3% donkey serum and 0.1% triton X-100 containing buffer. The following day, the sections were washed and incubated 2 hours at room temperature (in darkness) with Alexa Fluor®-conjugated secondary antibody diluted in 3% donkey serum and 0.1% triton X-100 at a concentration of 1:500. Slides were then cover-slipped using mounting medium (ProLong Gold antifade reagent, Life technologies, Thermo Fisher Scientific Inc.).

Avidin-biotin β-amyloid staining

This procedure has been detailed in previous reports [37, 38]. Briefly, sections of frontal and temporal cortex from the same patients used for ECM immunohistochemistry were cut at 6 µm thickness from formalin fixed, paraffin

embedded blocks and mounted on to glass slides (SuperFrost Plus Gold®, Thermo Fisher Scientific Inc.). Sections were firstly rehydrated in xylene followed by alcohols of decreasing concentration and distilled water. Sections were then subjected to chemical antigen retrieval (70% formic acid for 20 min at room temperature) and peroxidase activity was quenched (0.3% hydrogen peroxide in methanol for 30 min at room temperature). For all the following steps, horse serum (Vectastain Elite PK-6100, Vector Laboratories, CA, USA) was used as the blocking serum. The sections were next incubated for 1 hour at room temperature in mouse monoclonal antibody directed against Amyloid-β_{17-24} (4G8) (see Table 2) and then incubated with biotinylated secondary antibody for 30 min followed by 30 min incubation in ABC reagent (both Vectastain Elite PK-6100 mouse IgG). Sites of immunoreaction were visualized by incubating slices for 5 minutes in 3.3'-diaminobenzidine tetrahydrochloride (DAB), before lightly counterstaining with haematoxylin (Vector H-3401, Vector Laboratories). Finally, sections were dehydrated and mounted with Eukitt (Sigma) for analysis under the microscope.

Microscopic analysis and image quantification

Images were acquired using a 10x objective of an Olympus BX51 microscope and a QImaging Retiga 6000 color camera system. For each staining, image quantification was performed on one section per brain area per patient; all staining being performed on adjacent sections. For each section of frontal and temporal cortices, snapshots of five random fields of view of cortical grey matter were taken for each immunostaining. Although fields selected for image quantification were chosen at random, these were always taken from within the same gyral region (superior frontal gyrus or inferior temporal gyrus) in each case. This sampling procedure provided a histological reference point ensuring that broadly the same region of cortex was quantified in each patient for each antibody used. As all the ECM molecules reported here are expressed at the level of the basal membrane (BM) or by endothelial cells and not in the parenchyma, we assume that all reactions pattern are most certainly representative of changes at vascular level. Image analysis was performed using ImageJ software (ImageJ, U.S. National Institutes of Health, Bethesda, MD, USA, http://imagej.nih.gov/ij/). Firstly, all snapshots were converted to 8-bit black and white images. Then, a threshold by intensity and by size of object was applied to each image to remove any non-specific immunostaining. Finally, results were summarized

by averaging the total staining of the five snapshots for each antibody and expressed as area of positive staining per case and per mm^2 of tissue. Image acquisition and analysis were made blindly by a single observer. Higher magnification images (40x) were taken to present the perivascular staining pattern of each stain and are shown in Supplementary Figure 1.

Statistical analysis

A non-parametric one-way ANOVA (Kruskal-Wallis test) was used to compare the quantitative values of vascular staining for each antibody across the three groups in both frontal and temporal cortex. This was followed by a *post-hoc* analysis Dunn's test for multiple comparisons (the group sizes were not equal and all possible pairs were to be compared), and also to compare the mean age at death between groups. For correlations, the P-values in linear regression analysis were presented as well as the Pearson product-moment correlation coefficient r. Statistical significance was accepted at $P<0.05$ level. Statistical tests were performed using GraphPad Prism version 6.00 for Windows (GraphPad Software, CA, USA, www.graphpad.com).

Results

AD leads to changes in expression of ECM molecules

Subclinical AD and AD groups showed significantly higher levels of collagen IV (Figure 1) and perlecan (Figure 2) staining than the control group, for both frontal and temporal cortex, but no significant difference was observed between subclinical AD and AD groups.

Likewise, similar changes to those observed for collagen IV and perlecan were seen for fibronectin (Figure 3) ($P<0.05$), although variability within groups was higher than for collagen IV and perlecan which led to no significant difference between the AD group and the control group in the temporal cortex.

Staining for hPECAM was weaker than the other ECM immunostaining. Nonetheless, quantification of hPECAM staining in frontal and temporal cortex did not show any significant differences between groups (Figure 4).

AD leads to equivalent Aβ deposition between mild to moderate AD and moderate to severe AD groups

Similar to collagen IV, perlecan and fibronectin, Aβ deposition (represented by 4G8 immunostaining) was significantly higher in the subclinical AD and the AD groups versus the control group in both frontal and temporal cortex ($P<0.001$, for subclinical AD for both frontal and temporal cortex and for the AD group for frontal cortex, and $P<0.01$, for the AD group for temporal cortex), but did not differ significantly between subclinical AD and AD groups in either area (Figure 5).

Correlation between Aβ deposition and ECM components

There was a significant correlation between 4G8 staining and collagen IV staining in both frontal and temporal cortex (Figure 6a) ($P<0.0001$, $r=0.733$ and $P<0.0001$, $r=0.662$, for frontal and temporal cortex, respectively), as well as between 4G8 and perlecan (Figure 6b) ($P=0.0001$, $r=0.641$ and $P<0.0001$, $r=0.712$, for frontal and temporal cortex, respectively). Fibronectin and 4G8 staining were also correlated, but only in the temporal cortex (Figure 6c) ($P=0.1516$, $r=0.268$ and $P=0.0223$, $r=0.416$, for frontal and temporal cortex, respectively). Finally, consistent with the lack of changes in hPECAM staining, no correlation between Aβ deposition and hPECAM was seen (Figure 6d) ($P=0.4552$, $r=0.142$ and $P=0.5912$, $r=0.102$, for frontal and temporal cortex, respectively).

AD leads to a decrease in vessel density

A significant decrease in vWF staining was detected in the temporal cortex ($P<0.05$) (Figure 7) in the AD group when compared to the control and subclinical AD groups. A similar trend to decrease in vWF staining, although not significant ($P=0.0813$), was observed in the frontal cortex when comparing the control group with the subclinical AD and AD groups.

Discussion

In the present study, we have found early (i.e. in individuals with mild to moderate AD-type pathology; subclinical AD group) as well as late (i.e. in patients with established AD; Braak >4 group) increases in expression levels of collagen IV, perlecan and fibronectin as observed by immunohistochemistry. It must be noted that all changes described in this work were not visible on the standard hematoxylin and eosin staining (data not shown) and were only detectable by immunohistochemistry. Furthermore, Aβ accumulation is significantly increased in

subclinical AD patients (when compared to control subjects) with no further increase in later Braak stages. This latter finding is not totally unexpected since the subclinical AD cases are likely to be cases of probable AD, even though they may not have met yet the pathological criteria for definite AD. The similar patterns of Aβ accumulation and ECM changes logically lead to significant correlations between these parameters. Interestingly, we also show that these increase in ECM were not associated with an increase in vascular density, since vWF staining was actually unchanged in the frontal cortex and significantly decreased in temporal cortex of AD patients when compared to control subjects and subclinical AD.

The ECM provides a biochemical scaffolding that is essential for tissue elasticity, growth, remodelling, maintenance and stabilisation of tissue structures and represents a critical interface between tissue compartments providing essential attachment, survival, migration and functional clues for cells [20]. Over the last decades, several studies have disclosed changes in cell surface proteoglycans and/or ECM components in AD. Proteoglycans such as agrin, glypicans and syndecans, have been reported to be associated with senile plaques and NFT [41-43]. Berzin and co-workers [44] have shown that soluble agrin levels were significantly increased from Braak 3-4. Staining for a basement membrane-derived heparan sulfate proteoglycan was shown to be associated with diffuse plaques in both AD and Down's syndrome by Snow et al. [31], suggesting an early accumulation during plaque development. In an earlier study, Snow et al. [45], also demonstrated that proteoglycans co-localised with blood vessels in the brain parenchyma in non-affected areas while proteoglycan staining was lost in affected areas, suggesting a remodelling of the basement membrane and re-localisation of its constituent during amyloidogenesis. Here, we show that AD is associated with modifications in ECM components, as shown by a higher level of staining for these proteins. Our findings are in agreement with a previous study, which found a 55% increase of collagen IV content in cerebral microvessels in AD patients, compared to controls [26]. Other studies in AD [46, 47], and in transgenic animal models of AD [48, 49], also reported a thickening of the basement membrane together with an increase in collagen content. Moreover, alterations in microvascular morphology have been described in AD with a decrease in the diameter of capillaries correlating with a deteriorating cognitive status [50]. Decreased cerebrovascular volume, higher

levels of collagen IV and increased basement membrane thickness were also reported by Bourasset et al. [51] in the brains of 11 months old triple (APP×PS1×Tau) transgenic mice. Additionally, present data show higher levels in perlecan (as suggested by Kalaria and co-workers [26]) and fibronectin, which corroborates results from Lemańska-Perek and co-workers [33] in mild to moderate AD pathology, and reinforces the idea of a thicker basement membrane. These data further support the argument that the possible reduction of the cerebrovascular volume observed by Bouras et al. [50] and Bourasset et al. [51] could be the result of a thickening of the brain microvessels, or more specifically of their basement membrane.

Various processes may cause such changes in ECM in AD. One possible explanation for these ECM accumulations might lie with a reduction in brain proteolytic systems. The natural tissue endogenous inhibitors (TIMPs), as well as the matrix metalloproteinases (MMPs), are implicated in the regulation of ECM metabolism, and changes in activity of these proteases may contribute to vascular remodelling by modulating ECM components [52, 53]. Moreover, reports have shown an increase in levels of MMP-1 [54] or a decrease in MMP-9 [55] in brain, and Mroczko and co-workers [56] have shown an increase in MMP-3 and a decrease in MMP-9 in cerebrospinal fluid (CSF) of AD patients. Dysregulation of these proteases might result in a decreased turnover of the basement membrane with a consecutive build-up of ECM components and potential dysfunction of the blood-brain barrier (BBB). In fact, an increasing amount of evidence suggests that MMPs and TIMPs may play a crucial role in the pathogenesis of AD [21, 57, 58]. These reports together with our findings warrant further studies to elucidate the role of these proteases in pathophysiology of AD. On another hand, because grey matter atrophy has been previously reported in AD [59-62], we cannot rule out that some degree of grey matter shrinkage, leading to an increase in vessel density, could partly explain some of the increase in vessel components we have observed. However, this seems unlikely for several reasons. Firstly, our vWF staining data, a commonly used endothelial cell marker, suggests that late stage AD patients have no change, or even a decrease in vascular density in frontal and temporal cortex, respectively. Such decreases in capillary density are in agreement with previous studies [63-66]. Secondly, the magnitude of the component increase measured in the present study

(+51-59% for collagen IV (see Figure 1), +23-79% for perlecan (see Figure 2) and +96-112% for fibronectin (see Figure 3)) is far greater than the degree of grey matter shrinkage, commonly reported to be around 5-15% in terms of volume in the frontal and temporal areas [59-62]. Finally, angiogenesis could be another explanation for an increase in vascular components, but to date there is only little evidence supporting this. For example, Desai and collaborators [67] showed an increased in integrin $\alpha_V\beta_3$ in the brain in AD, but this was associated with an increase in blood vessel density only in the hippocampus, an area which was not included in the present study. Accordingly, our first hypothesis based on a potential dysfunction of the proteolytic systems seems to be the most likely explanation for the increase of ECM components expression per vessel.

In our study, we did not find any difference in hPECAM staining between the different Braak stages. hPECAM is a transmembrane immunoglobulin expressed by endothelial cells, where it is localised at the intercellular points of contacts, and by leukocytes and platelets [68], which in turn are known to play a role in Aβ deposition and inflammatory processes [69]. Plasma levels of hPECAM were found to be higher in AD patients versus controls [69-71], but no significant differences between the moderate to severe AD group and the mild AD group could be identified [71]. The difference between these reports and our present results may be due to a bias in our control group in which cases with Braak stage ≤2 and those with Braak 0 (ie 'true' control cases) were pooled. However, it is more likely that hPECAM is released into the circulation rather than accumulating in the basement membrane, hence explaining why plasma levels are higher whereas vascular levels remain fairly constant. Again, roles of the MMPs and TIMPs in the regulation of the expression of the junctional adhesion protein need to be considered [72].

Finally, we found positive, although modest (r=0.41-0.773), correlations between Aβ deposition and changes in ECM components. Overall, this result is in agreement with previous findings reporting an association between vascular Aβ deposition and alterations of the cerebral vasculature such as smooth muscle loss [73] together with collagen IV deposition [30], apoptosis of cerebral vascular cells [74]. Altogether, these observations and previous reports support the concept that vascular changes are concomitant to disease progression, whether they are causative/contributing or simply consequences of the disease remains to be investigated.

In conclusion, our present results suggest that changes in ECM components could be potential biomarkers for investigational studies, at plasma level or using imaging techniques, in AD from early Braak stages, due to their alterations from Braak >2, or in animal models to determine the time-course of these changes at vascular level and the potential causality between them and AD pathology. Indeed, the recurrent problem is that the diagnosis of AD is based on a combination of cognitive tests, imaging and exclusion of other neurological disorders. Unfortunately, in most cases, the diagnosis is ascertained only when the disease has already been progressing for many years, and cases will likely exceed Braak stage 2 when diagnosed. Accordingly, our study supports the need to find molecular markers that will help diagnose AD as early as possible, as blood plasma measures [75], and to provide objective and reliable measures of disease progression. Imaging agents to measure ECM molecules in human patients could be useful, but these would need to access the basement membrane, which is beyond the BBB formed by tight junctions between endothelial cells, and therefore such approach would be very challenging. Plasma measures of ECM components seem better adapted for potential use as biomarkers to predict development of AD. Finally, it has been shown that ECM molecules may also represent potential therapeutic targets for stroke or AD [76, 77]; therefore our present data could be useful in defining new therapeutic strategies.

Acknowledgements

This study was supported by the European Union's Seventh Framework Programme (FP7/2007-2013) under grant agreement n°HEALTH-F2-2011-278850 (INMiND). Tissue samples were supplied by The Manchester Brain Bank, which is part of the Brains for Dementia Research Programme, jointly funded by Alzheimer's Society and Alzheimer's Research UK.

Individual contribution of the authors: FXL performed the experiments and analysed all the data; DMM performed the neuropathological assessment of the patients and provided his expertise as neuropathologist during data analysis; ACR performed the immunohistochemistry for the amyloid plaques and provided technical support at the Manchester Brain Bank; EP contributed to the study design; HB designed the study and data analysis methods and oversaw the experiments and data analysis and is

the budget holder of the grant funding this project. FXL, DMM, EP and HB wrote the manuscript.

Conflict of interests

The authors have no conflict of interests to report.

References

1 Crews L, Masliah E. Molecular mechanisms of neurodegeneration in Alzheimer's disease. Hum Mol Genet 2010;19(R1): R12-20
2 Braak H, Braak E. Neuropathological stageing of Alzheimer-related changes. Acta Neuropathol 1991;82(4): 239-59
3 Thal DR, Rub U, Orantes M, Braak H. Phases of A beta-deposition in the human brain and its relevance for the development of AD. Neurology 2002;58(12): 1791-800
4 Ariga T, Miyatake T, Yu RK. Role of proteoglycans and glycosaminoglycans in the pathogenesis of Alzheimer's disease and related disorders: amyloidogenesis and therapeutic strategies--a review. J Neurosci Res 2010;88(11): 2303-15
5 Genedani S, Agnati LF, Leo G, Buzzega D, Maccari F, Carone C, Andreoli N, Filaferro M, Volpi N. beta-Amyloid fibrillation and/or hyperhomocysteinemia modify striatal patterns of hyaluronic acid and dermatan sulfate: Possible role in the pathogenesis of Alzheimer's disease. Curr Alzheimer Res 2010;7(2): 150-7
6 Alexandrescu AT. Amyloid accomplices and enforcers. Protein Sci 2005;14(1): 1-12
7 Ancsin JB. Amyloidogenesis: historical and modern observations point to heparan sulfate proteoglycans as a major culprit. Amyloid 2003;10(2): 67-79
8 Brandan E, Inestrosa NC. Extracellular matrix components and amyloid in neuritic plaques of Alzheimer's disease. Gen Pharmacol 1993;24(5): 1063-8
9 Caltagarone J, Jing Z, Bowser R. Focal adhesions regulate Abeta signaling and cell death in Alzheimer's disease. Biochim Biophys Acta 2007;1772(4): 438-45
10 Fukuchi K, Hart M, Li L. Alzheimer's disease and heparan sulfate proteoglycan. Front Biosci 1998;3(d327-37
11 Hirschfield GM, Hawkins PN. Amyloidosis: new strategies for treatment. Int J Biochem Cell Biol 2003;35(12): 1608-13
12 Ajmo JM, Bailey LA, Howell MD, Cortez LK, Pennypacker KR, Mehta HN, Morgan D, Gordon MN, Gottschall PE. Abnormal post-translational and extracellular processing of brevican in plaque-bearing mice over-expressing APPsw. J Neurochem 2010;113(3): 784-95
13 Sykova E, Vorisek I, Antonova T, Mazel T, Meyer-Luehmann M, Jucker M, Hajek M, Ort M, Bures J. Changes in extracellular space size and geometry in APP23 transgenic mice: a model of Alzheimer's disease. Proc Natl Acad Sci U S A 2005;102(2): 479-84
14 Frantz C, Stewart KM, Weaver VM. The extracellular matrix at a glance. J Cell Sci 2010;123(Pt 24): 4195-200
15 Lau LW, Cua R, Keough MB, Haylock-Jacobs S, Yong VW. Pathophysiology of the brain extracellular matrix: a new target for remyelination. Nat Rev Neurosci 2013;14(10): 722-9

16 Rozario T, DeSimone DW. The extracellular matrix in development and morphogenesis: a dynamic view. Dev Biol 2010;341(1): 126-40
17 Farach-Carson MC, Warren CR, Harrington DA, Carson DD. Border patrol: insights into the unique role of perlecan/heparan sulfate proteoglycan 2 at cell and tissue borders. Matrix Biol 2014;34(64-79
18 Wong CW, Wiedle G, Ballestrem C, Wehrle-Haller B, Etteldorf S, Bruckner M, Engelhardt B, Gisler RH, Imhof BA. PECAM-1/CD31 trans-homophilic binding at the intercellular junctions is independent of its cytoplasmic domain; evidence for heterophilic interaction with integrin alphavbeta3 in Cis. Mol Biol Cell 2000;11(9): 3109-21
19 Collins C, Guilluy C, Welch C, O'Brien ET, Hahn K, Superfine R, Burridge K, Tzima E. Localized tensional forces on PECAM-1 elicit a global mechanotransduction response via the integrin-RhoA pathway. Curr Biol 2012;22(22): 2087-94
20 Kurtz A, Oh SJ. Age related changes of the extracellular matrix and stem cell maintenance. Prev Med 2012;54 Suppl(S50-6
21 Morawski M, Filippov M, Tzinia A, Tsilibary E, Vargova L. ECM in brain aging and dementia. Prog Brain Res 2014;214(207-27
22 Dityatev A, Schachner M, Sonderegger P. The dual role of the extracellular matrix in synaptic plasticity and homeostasis. Nat Rev Neurosci 2010;11(11): 735-46
23 Dityatev A, Seidenbecher CI, Schachner M. Compartmentalization from the outside: the extracellular matrix and functional microdomains in the brain. Trends Neurosci 2010;33(11): 503-12
24 Dityatev A, Rusakov DA. Molecular signals of plasticity at the tetrapartite synapse. Curr Opin Neurobiol 2011;21(2): 353-9
25 Dityatev A, Schachner M. Extracellular matrix molecules and synaptic plasticity. Nat Rev Neurosci 2003;4(6): 456-68
26 Kalaria RN, Pax AB. Increased collagen content of cerebral microvessels in Alzheimer's disease. Brain Res 1995;705(1-2): 349-52
27 Farkas E, De Jong GI, de Vos RA, Jansen Steur EN, Luiten PG. Pathological features of cerebral cortical capillaries are doubled in Alzheimer's disease and Parkinson's disease. Acta Neuropathol 2000;100(4): 395-402
28 Challa VR, Thore CR, Moody DM, Anstrom JA, Brown WR. Increase of white matter string vessels in Alzheimer's disease. J Alzheimers Dis 2004;6(4): 379-83; discussion 443-9
29 Christov A, Ottman J, Hamdheydari L, Grammas P. Structural changes in Alzheimer's disease brain microvessels. Curr Alzheimer Res 2008;5(4): 392-5
30 Tian J, Shi J, Smallman R, Iwatsubo T, Mann DM. Relationships in Alzheimer's disease between the extent of Abeta deposition in cerebral blood vessel walls, as cerebral amyloid angiopathy, and the amount of cerebrovascular smooth muscle cells and collagen. Neuropathol Appl Neurobiol 2006;32(3): 332-40
31 Snow AD, Mar H, Nochlin D, Sekiguchi RT, Kimata K, Koike Y, Wight TN. Early accumulation of heparan sulfate in neurons and in the beta-amyloid protein-containing lesions of Alzheimer's disease and Down's syndrome. Am J Pathol 1990;137(5): 1253-70
32 Maresh GA, Erezyilmaz D, Murry CE, Nochlin D, Snow AD. Detection and quantitation of perlecan mRNA levels in Alzheimer's disease and normal aged hippocampus by competitive reverse transcription-polymerase chain reaction. J Neurochem 1996;67(3): 1132-44

33 Lemanska-Perek A, Leszek J, Krzyzanowska-Golab D, Radzik J, Katnik-Prastowska I. Molecular status of plasma fibronectin as an additional biomarker for assessment of Alzheimer's dementia risk. Dement Geriatr Cogn Disord 2009;28(4): 338-42
34 Muenchhoff J, Poljak A, Song F, Raftery M, Brodaty H, Duncan M, McEvoy M, Attia J, Schofield PW, Sachdev PS. Plasma protein profiling of mild cognitive impairment and Alzheimer's disease across two independent cohorts. J Alzheimers Dis 2015;43(4): 1355-73
35 Rattan SI, Rasmussen LM, Bjerring P, Bhatia P, Clark BF. Unchanged concentrations of plasma fibronectin in Alzheimer's disease. J Clin Pathol 1988;41(4): 476
36 Zanetta L, Marcus SG, Vasile J, Dobryansky M, Cohen H, Eng K, Shamamian P, Mignatti P. Expression of Von Willebrand factor, an endothelial cell marker, is up-regulated by angiogenesis factors: a potential method for objective assessment of tumor angiogenesis. Int J Cancer 2000;85(2): 281-8
37 Allen N, Robinson AC, Snowden J, Davidson YS, Mann DM. Patterns of cerebral amyloid angiopathy define histopathological phenotypes in Alzheimer's disease. Neuropathol Appl Neurobiol 2014;40(2): 136-48
38 Lant SB, Robinson AC, Thompson JC, Rollinson S, Pickering-Brown S, Snowden JS, Davidson YS, Gerhard A, Mann DM. Patterns of microglial cell activation in frontotemporal lobar degeneration. Neuropathol Appl Neurobiol 2014;40(6): 686-96
39 Hyman BT, Phelps CH, Beach TG, Bigio EH, Cairns NJ, Carrillo MC, Dickson DW, Duyckaerts C, Frosch MP, Masliah E, Mirra SS, Nelson PT, Schneider JA, Thal DR, Thies B, Trojanowski JQ, Vinters HV, Montine TJ. National Institute on Aging-Alzheimer's Association guidelines for the neuropathologic assessment of Alzheimer's disease. Alzheimers Dement 2012;8(1): 1-13
40 Mirra SS, Heyman A, McKeel D, Sumi SM, Crain BJ, Brownlee LM, Vogel FS, Hughes JP, van Belle G, Berg L. The Consortium to Establish a Registry for Alzheimer's Disease (CERAD). Part II. Standardization of the neuropathologic assessment of Alzheimer's disease. Neurology 1991;41(4): 479-86
41 Perry G, Siedlak SL, Richey P, Kawai M, Cras P, Kalaria RN, Galloway PG, Scardina JM, Cordell B, Greenberg BD, et al. Association of heparan sulfate proteoglycan with the neurofibrillary tangles of Alzheimer's disease. J Neurosci 1991;11(11): 3679-83
42 van Horssen J, Otte-Holler I, David G, Maat-Schieman ML, van den Heuvel LP, Wesseling P, de Waal RM, Verbeek MM. Heparan sulfate proteoglycan expression in cerebrovascular amyloid beta deposits in Alzheimer's disease and hereditary cerebral hemorrhage with amyloidosis (Dutch) brains. Acta Neuropathol 2001;102(6): 604-14
43 Verbeek MM, Otte-Holler I, van den Born J, van den Heuvel LP, David G, Wesseling P, de Waal RM. Agrin is a major heparan sulfate proteoglycan accumulating in Alzheimer's disease brain. Am J Pathol 1999;155(6): 2115-25
44 Berzin TM, Zipser BD, Rafii MS, Kuo-Leblanc V, Yancopoulos GD, Glass DJ, Fallon JR, Stopa EG. Agrin and microvascular damage in Alzheimer's disease. Neurobiol Aging 2000;21(2): 349-55
45 Snow AD, Mar H, Nochlin D, Kimata K, Kato M, Suzuki S, Hassell J, Wight TN. The presence of heparan sulfate proteoglycans in the neuritic plaques and congophilic angiopathy in Alzheimer's disease. Am J Pathol 1988;133(3): 456-63

46 Tong XK, Nicolakakis N, Kocharyan A, Hamel E. Vascular remodeling versus amyloid beta-induced oxidative stress in the cerebrovascular dysfunctions associated with Alzheimer's disease. J Neurosci 2005;25(48): 11165-74
47 Zarow C, Barron E, Chui HC, Perlmutter LS. Vascular basement membrane pathology and Alzheimer's disease. Ann N Y Acad Sci 1997;826(147-60
48 Rockenstein E, Adame A, Mante M, Larrea G, Crews L, Windisch M, Moessler H, Masliah E. Amelioration of the cerebrovascular amyloidosis in a transgenic model of Alzheimer's disease with the neurotrophic compound cerebrolysin. J Neural Transm 2005;112(2): 269-82
49 Thal DR, Capetillo-Zarate E, Larionov S, Staufenbiel M, Zurbruegg S, Beckmann N. Capillary cerebral amyloid angiopathy is associated with vessel occlusion and cerebral blood flow disturbances. Neurobiol Aging 2009;30(12): 1936-48
50 Bouras C, Kovari E, Herrmann FR, Rivara CB, Bailey TL, von Gunten A, Hof PR, Giannakopoulos P. Stereologic analysis of microvascular morphology in the elderly: Alzheimer disease pathology and cognitive status. J Neuropathol Exp Neurol 2006;65(3): 235-44
51 Bourasset F, Ouellet M, Tremblay C, Julien C, Do TM, Oddo S, LaFerla F, Calon F. Reduction of the cerebrovascular volume in a transgenic mouse model of Alzheimer's disease. Neuropharmacology 2009;56(4): 808-13
52 Burggraf D, Martens HK, Jager G, Hamann GF. Recombinant human tissue plasminogen activator protects the basal lamina in experimental focal cerebral ischemia. Thromb Haemost 2003;89(6): 1072-80
53 Pfefferkorn T, Wiessner C, Allegrini PR, Staufer B, Vosko MR, Liebetrau M, Bueltemeier G, Kloss CU, Hamann GF. Plasminogen activation in experimental permanent focal cerebral ischemia. Brain Res 2000;882(1-2): 19-25
54 Leake A, Morris CM, Whateley J. Brain matrix metalloproteinase 1 levels are elevated in Alzheimer's disease. Neurosci Lett 2000;291(3): 201-3
55 Horstmann S, Budig L, Gardner H, Koziol J, Deuschle M, Schilling C, Wagner S. Matrix metalloproteinases in peripheral blood and cerebrospinal fluid in patients with Alzheimer's disease. Int Psychogeriatr 2010;22(6): 966-72
56 Mroczko B, Groblewska M, Zboch M, Kulczynska A, Koper OM, Szmitkowski M, Kornhuber J, Lewczuk P. Concentrations of matrix metalloproteinases and their tissue inhibitors in the cerebrospinal fluid of patients with Alzheimer's disease. J Alzheimers Dis 2014;40(2): 351-7
57 Bonneh-Barkay D, Wiley CA. Brain extracellular matrix in neurodegeneration. Brain Pathol 2009;19(4): 573-85
58 Stomrud E, Bjorkqvist M, Janciauskiene S, Minthon L, Hansson O. Alterations of matrix metalloproteinases in the healthy elderly with increased risk of prodromal Alzheimer's disease. Alzheimers Res Ther 2010;2(3): 20
59 Frings L, Yew B, Flanagan E, Lam BY, Hull M, Huppertz HJ, Hodges JR, Hornberger M. Longitudinal grey and white matter changes in frontotemporal dementia and Alzheimer's disease. PLoS One 2014;9(3): e90814
60 Karas GB, Scheltens P, Rombouts SA, Visser PJ, van Schijndel RA, Fox NC, Barkhof F. Global and local gray matter loss in mild cognitive impairment and Alzheimer's disease. Neuroimage 2004;23(2): 708-16
61 Mann DM. The topographic distribution of brain atrophy in Alzheimer's disease. Acta Neuropathol 1991;83(1): 81-6

62 Rusinek H, de Leon MJ, George AE, Stylopoulos LA, Chandra R, Smith G, Rand T, Mourino M, Kowalski H. Alzheimer disease: measuring loss of cerebral gray matter with MR imaging. Radiology 1991;178(1): 109-14
63 Bell MA, Ball MJ. Morphometric comparison of hippocampal microvasculature in ageing and demented people: diameters and densities. Acta Neuropathol 1981;53(4): 299-318
64 Bell MA, Ball MJ. The correlation of vascular capacity with the parenchymal lesions of Alzheimer's disease. Can J Neurol Sci 1986;13(4 Suppl): 456-61
65 Brown WR, Moody DM, Thore CR, Challa VR, Anstrom JA. Vascular dementia in leukoaraiosis may be a consequence of capillary loss not only in the lesions, but in normal-appearing white matter and cortex as well. J Neurol Sci 2007;257(1-2): 62-6
66 Fischer VW, Siddiqi A, Yusufaly Y. Altered angioarchitecture in selected areas of brains with Alzheimer's disease. Acta Neuropathol 1990;79(6): 672-9
67 Desai BS, Schneider JA, Li JL, Carvey PM, Hendey B. Evidence of angiogenic vessels in Alzheimer's disease. J Neural Transm 2009;116(5): 587-97
68 Bazzoni G, Dejana E. Endothelial cell-to-cell junctions: molecular organization and role in vascular homeostasis. Physiol Rev 2004;84(3): 869-901
69 Casoli T, Di Stefano G, Balietti M, Solazzi M, Giorgetti B, Fattoretti P. Peripheral inflammatory biomarkers of Alzheimer's disease: the role of platelets. Biogerontology 2010;11(5): 627-33
70 Nielsen HM, Londos E, Minthon L, Janciauskiene SM. Soluble adhesion molecules and angiotensin-converting enzyme in dementia. Neurobiol Dis 2007;26(1): 27-35
71 Xue S, Cai X, Li W, Zhang Z, Dong W, Hui G. Elevated plasma endothelial microparticles in Alzheimer's disease. Dement Geriatr Cogn Disord 2012;34(3-4): 174-80
72 Akahane T, Akahane M, Shah A, Connor CM, Thorgeirsson UP. TIMP-1 inhibits microvascular endothelial cell migration by MMP-dependent and MMP-independent mechanisms. Exp Cell Res 2004;301(2): 158-67
73 Haglund M, Kalaria R, Slade JY, Englund E. Differential deposition of amyloid beta peptides in cerebral amyloid angiopathy associated with Alzheimer's disease and vascular dementia. Acta Neuropathol 2006;111(5): 430-5
74 Miao J, Xu F, Davis J, Otte-Holler I, Verbeek MM, Van Nostrand WE. Cerebral microvascular amyloid beta protein deposition induces vascular degeneration and neuroinflammation in transgenic mice expressing human vasculotropic mutant amyloid beta precursor protein. Am J Pathol 2005;167(2): 505-15
75 Ray S, Britschgi M, Herbert C, Takeda-Uchimura Y, Boxer A, Blennow K, Friedman LF, Galasko DR, Jutel M, Karydas A, Kaye JA, Leszek J, Miller BL, Minthon L, Quinn JF, Rabinovici GD, Robinson WH, Sabbagh MN, So YT, Sparks DL, Tabaton M, Tinklenberg J, Yesavage JA, Tibshirani R, Wyss-Coray T. Classification and prediction of clinical Alzheimer's diagnosis based on plasma signaling proteins. Nat Med 2007;13(11): 1359-62
76 Marcelo A, Bix G. Investigating the role of perlecan domain V in post-ischemic cerebral angiogenesis. Methods Mol Biol 2014;1135(331-41
77 Kalinowska A, Losy J. PECAM-1, a key player in neuroinflammation. Eur J Neurol 2006;13(12): 1284-90

Figure legends

Figure 1. Quantification of collagen IV staining per mm^2 in the subcortical grey matter of control subjects (Braak ≤2, n=12), subclinical AD (Braak >2 & ≤4, n=10) and moderate to severe AD patients (Braak >4, n=8) in frontal cortex (left panel) and in temporal cortex (right panel). Area of collagen IV staining per mm^2 for each case is shown as circle for Braak ≤2, square for Braak >2 & ≤4 and triangle for Braak >4, as well as the mean ± standard deviation. Microscopic images show representative examples of immunostaining for each group (Scale bars represent 0.4mm) highlighting the significant increase in collagen IV immunostaining with the progression towards more advanced Braak stages. Data were analysed by a non-parametric Kruskal-Wallis test (P<0.0001, for both frontal and temporal cortex) with a Dunn's *post-hoc* analysis (***P<0.001).

Figure 2. Quantification of perlecan staining per mm^2 in the subcortical grey matter of control subjects (Braak ≤2, n=12), subclinical AD (Braak >2 & ≤4, n=10) and moderate to severe AD patients (Braak >4, n=8) in frontal cortex (left panel) and in temporal cortex (right panel). The perlecan staining per mm^2 for each case is shown as circle for Braak ≤2, square for Braak >2 & ≤4 and triangle for Braak >4, as well as the mean ± standard deviation. Microscopic images show representative examples of immunostaining for each group (Scale bars represent 0.4mm) highlighting the significant increase in perlecan immunostaining with the progression towards more advanced Braak stages. Data were analysed by a non-parametric Kruskal-Wallis test (P=0.0003 and P<0.0001 for frontal and temporal cortex, respectively) with a Dunn's *post-hoc* analysis (**P<0.01, ***P<0.001).

Figure 3. Quantification of fibronectin staining per mm^2 in the subcortical grey matter of control subjects (Braak ≤2, n=12), subclinical AD (Braak >2 & ≤4, n=10) and moderate to severe AD patients (Braak >4, n=8) in frontal cortex (left panel) and in temporal cortex (right panel). The fibronectin staining per mm^2 for each case is shown as circle for Braak ≤2, square for Braak >2 & ≤4 and triangle for Braak >4, as well as the mean ± standard deviation. Microscopic images show representative examples of immunostaining for each group (Scale bars represent 0.4mm) highlighting the significant increase in fibronectin immunostaining with the progression towards more advanced Braak stages. Data were analysed by a non-parametric Kruskal-Wallis test (P=0.0140 and P=0.0069 for frontal and temporal cortex, respectively) with a Dunn's *post-hoc* analysis (*P<0.05).

Figure 4. Quantification of hPECAM staining per mm^2 in the subcortical grey matter of control subjects (Braak ≤2, n=12), subclinical AD (Braak >2 & ≤4, n=10) and moderate to severe AD patients (Braak >4, n=8) in frontal cortex (left panel) and in temporal cortex (right panel). The hPECAM staining per mm^2 for each case is shown as circle for Braak ≤2, square for Braak >2 & ≤4 and triangle for Braak >4, as well as the mean ± standard deviation. Microscopic images show representative examples of immunostaining for each group (Scale bars represent 0.4mm) showing low level of immunostaining and the lack of difference between the different Braak stages. Data were analysed by a non-parametric Kruskal-Wallis test (P=0.3100 and P=0.8661 for frontal and temporal cortex, respectively) with a Dunn's *post-hoc* analysis.

Figure 5. Quantification of 4G8 staining per mm^2 in the subcortical grey matter of control subjects (Braak ≤2, n=12), subclinical AD (Braak >2 & ≤4, n=10) and moderate to severe AD patients (Braak >4, n=8) in frontal cortex (left panel) and in temporal cortex (right panel). The 4G8 staining per mm^2 for each case is shown as circle for Braak ≤2, square for Braak >2 & ≤4 and triangle for Braak >4, as well as the mean ± standard deviation. Microscopic images show representative examples of immunostaining for each group (Scale bars represent 0.4mm) showing a significant increase in amyloid immunostaining with the progression towards more advanced Braak stages. Data were analysed by a non-parametric Kruskal-Wallis test (P<0.0001, for both frontal and temporal cortex) with a Dunn's *post-hoc* analysis (**P<0.01, ***P<0.001).

Figure 6. Correlation plots between amyloid-β (4G8) immunostaining and the different components staining per mm^2 in the subcortical grey matter in frontal cortex (left panel) and in temporal cortex (right panel): a) collagen IV, b) perlecan, c) fibronectin, d) hPECAM. The graphs present the data points (squares, n=30) and a linear regression line (thick line). The P-value as well as the Pearson product-moment correlation coefficient is shown in each graph.

Figure 7. Quantification of vWF staining per mm^2 in the subcortical grey matter of control subjects (Braak ≤2, n=12), subclinical AD (Braak >2 & ≤4, n=10) and moderate to severe AD patients (Braak >4, n=8) in frontal cortex (left panel) and in temporal cortex (right panel). The vWF staining per mm^2 for each case is shown as circle for Braak ≤2, square for Braak >2 & ≤4 and triangle for Braak >4, as well as the mean ± standard deviation. Microscopic images show representative examples of immunostaining for each group (Scale bars represent 0.4mm) illustrating the lack of changes in vessel density in the frontal cortex across pathological stages and a significant decrease vessel density in the temporal cortex in the advanced AD patients (Braak stage >4).. Data were analysed by a non-parametric Kruskal-Wallis test (P=0.0813 for both frontal and P=0.0111 for temporal cortex) with a Dunn's *post-hoc* analysis (*P<0.05). Scale bars represent 0.4mm.

Supplementary Figure 1. Visualisation of the different immunostaining (collagen IV, perlecan, fibronectin, hPECAM and vWF, from top to bottom) at magnification 10x (left panel, scale bars represent 0.4mm) and magnification 40x (right panel, scale bars represent 0.1mm).

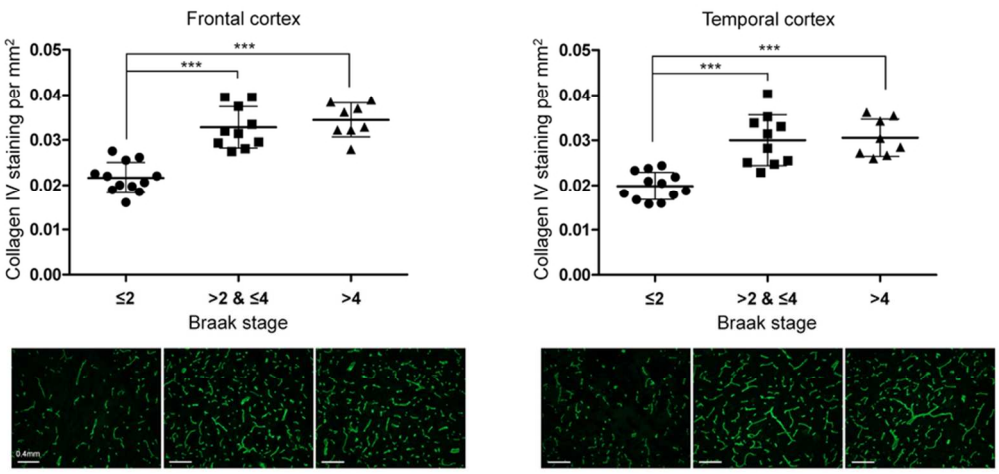

Quantification of collagen IV staining per mm2 in the subcortical grey matter of control subjects (Braak ≤2, n=12), mild to moderate (Braak >2 & ≤4, n=10) and moderate to severe AD patients (Braak >4, n=8) in frontal cortex (left panel) and in temporal cortex (right panel). The collagen IV staining per mm2 for each case is shown as circle for Braak ≤2, square for Braak >2 & ≤4 and triangle for Braak >4, as well as the mean ± standard deviation, in addition to representative examples of immunostaining for the different groups. Data were analysed by a non-parametric Kruskal-Wallis test (P<0.0001, for both frontal and temporal cortex) with a Dunn's post-hoc analysis (***P<0.001). Scale bars represent 0.4mm.
80x37mm (300 x 300 DPI)

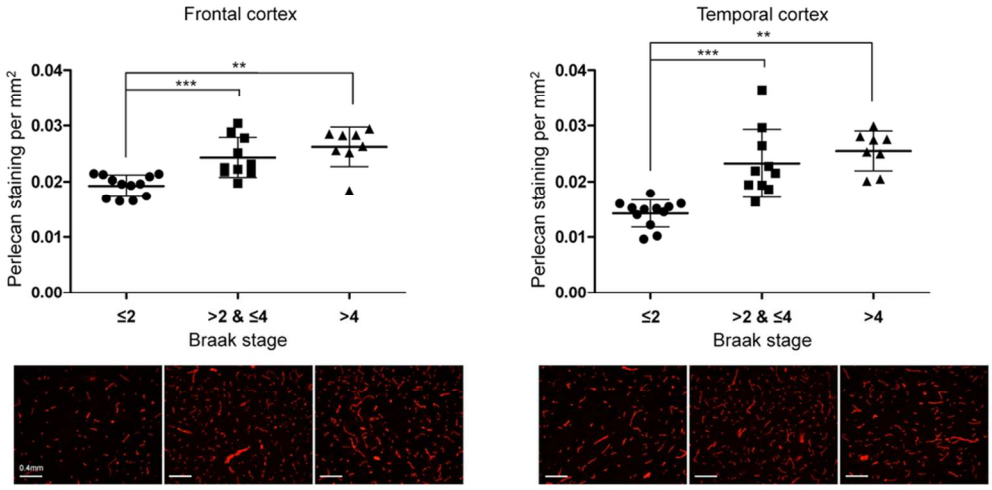

Quantification of perlecan staining per mm2 in the subcortical grey matter of control subjects (Braak ≤2, n=12), mild to moderate (Braak >2 & ≤4, n=10) and moderate to severe AD patients (Braak >4, n=8) in frontal cortex (left panel) and in temporal cortex (right panel). The perlecan staining per mm2 for each case is shown as circle for Braak ≤2, square for Braak >2 & ≤4 and triangle for Braak >4, as well as the mean ± standard deviation, in addition to representative examples of immunostaining for the different groups. Data were analysed by a non-parametric Kruskal-Wallis test (P=0.0003 and P<0.0001 for frontal and temporal cortex, respectively) with a Dunn's post-hoc analysis (**P<0.01, ***P<0.001). Scale bars represent 0.4mm.

84x41mm (300 x 300 DPI)

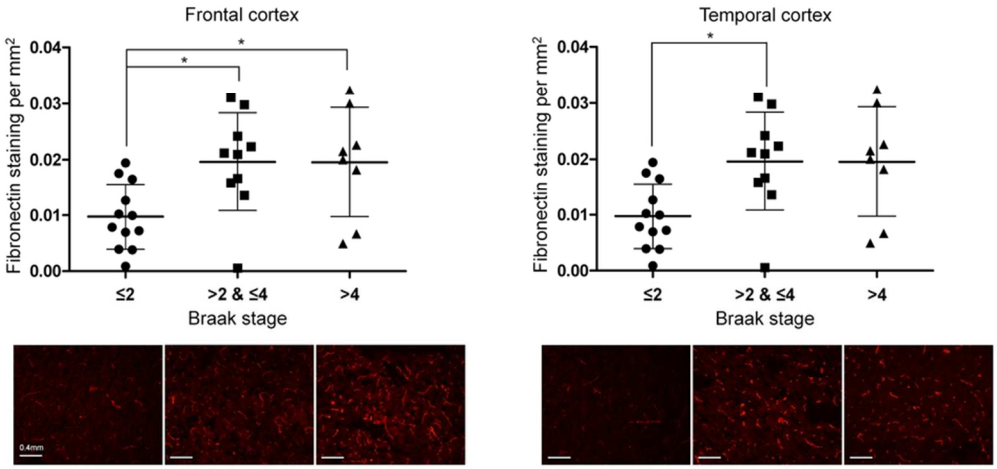

Quantification of fibronectin staining per mm2 in the subcortical grey matter of control subjects (Braak ≤2, n=12), mild to moderate (Braak >2 & ≤4, n=10) and moderate to severe AD patients (Braak >4, n=8) in frontal cortex (left panel) and in temporal cortex (right panel). The fibronectin staining per mm2 for each case is shown as circle for Braak ≤2, square for Braak >2 & ≤4 and triangle for Braak >4, as well as the mean ± standard deviation, in addition to representative examples of immunostaining for the different groups. Data were analysed by a non-parametric Kruskal-Wallis test (P=0.0140 and P=0.0069 for frontal and temporal cortex, respectively) with a Dunn's post-hoc analysis (*P<0.05). Scale bars represent 0.4mm.
80x38mm (300 x 300 DPI)

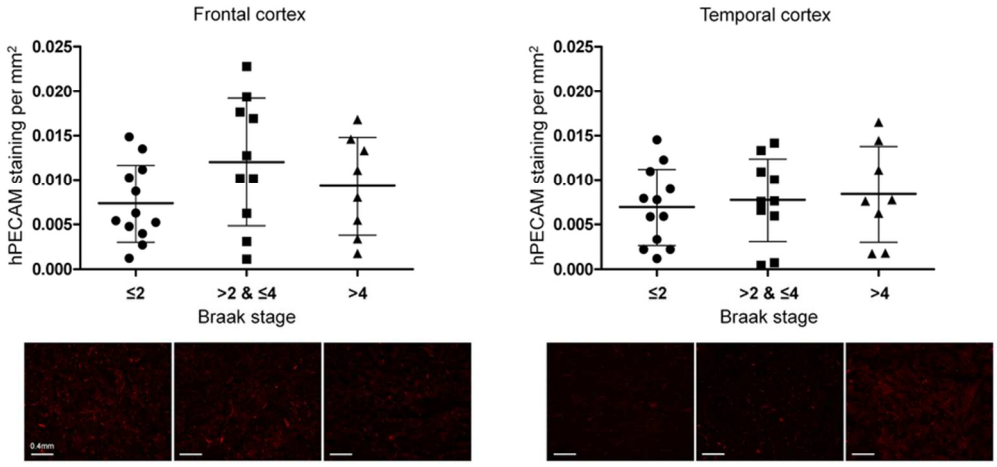

Quantification of hPECAM staining per mm2 in the subcortical grey matter of control subjects (Braak ≤2, n=12), mild to moderate (Braak >2 & ≤4, n=10) and moderate to severe AD patients (Braak >4, n=8) in frontal cortex (left panel) and in temporal cortex (right panel). The hPECAM staining per mm2 for each case is shown as circle for Braak ≤2, square for Braak >2 & ≤4 and triangle for Braak >4, as well as the mean ± standard deviation, in addition to representative examples of immunostaining for the different groups. Data were analysed by a non-parametric Kruskal-Wallis test (P=0.3100 and P=0.8661 for frontal and temporal cortex, respectively) with a Dunn's post-hoc analysis. Scale bars represent 0.4mm.
78x36mm (300 x 300 DPI)

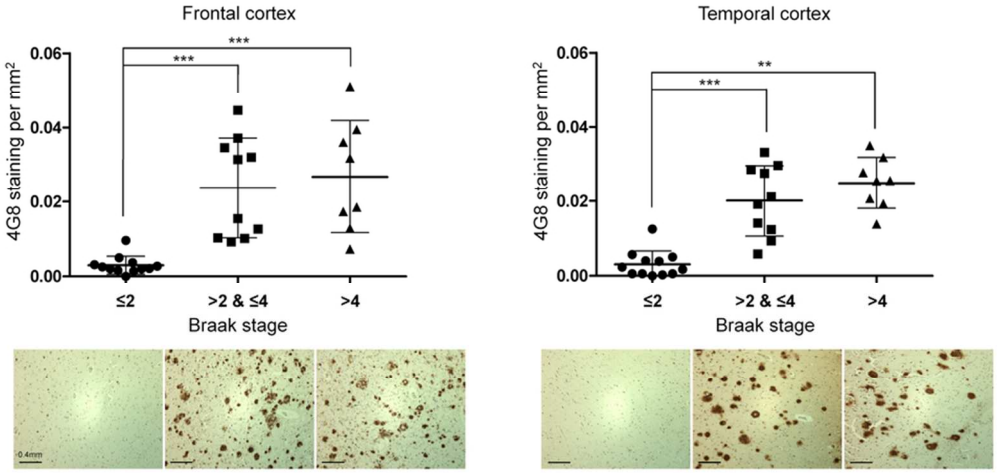

Quantification of 4G8 staining per mm2 in the subcortical grey matter of control subjects (Braak ≤2, n=12), mild to moderate (Braak >2 & ≤4, n=10) and moderate to severe AD patients (Braak >4, n=8) in frontal cortex (left panel) and in temporal cortex (right panel). The 4G8 staining per mm2 for each case is shown as circle for Braak ≤2, square for Braak >2 & ≤4 and triangle for Braak >4, as well as the mean ± standard deviation, in addition to representative examples of immunostaining for the different groups. Data were analysed by a non-parametric Kruskal-Wallis test (P<0.0001, for both frontal and temporal cortex) with a Dunn's post-hoc analysis (**P<0.01, ***P<0.001). Scale bars represent 0.4mm.
81x38mm (300 x 300 DPI)

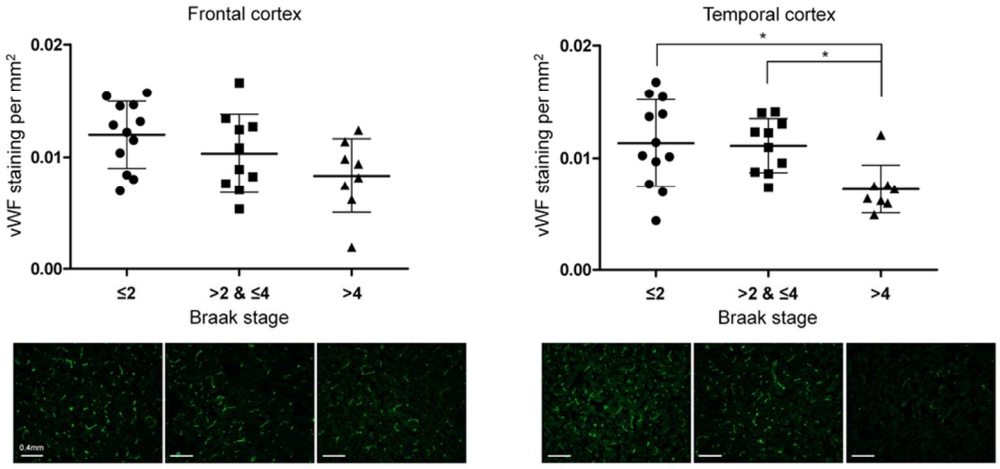

Quantification of vWF staining per mm2 in the subcortical grey matter of control subjects (Braak ≤2, n=12), mild to moderate (Braak >2 & ≤4, n=10) and moderate to severe AD patients (Braak >4, n=8) in frontal cortex (left panel) and in temporal cortex (right panel). The vWF staining per mm2 for each case is shown as circle for Braak ≤2, square for Braak >2 & ≤4 and triangle for Braak >4, as well as the mean ± standard deviation, in addition to representative examples of immunostaining for the different groups. Data were analysed by a non-parametric Kruskal-Wallis test (P=0.0813 for both frontal and P=0.0111 for temporal cortex) with a Dunn's post-hoc analysis (*P<0.05). Scale bars represent 0.4mm.
81x38mm (300 x 300 DPI)

Table 1

Clinical summary of autopsy cases

Case no.	Gender	Age of death (years)	PM delay (hours)	Principal pathological diagnosis	Age of disease onset (years)	Braak stage
1	M	54	37	Normal brain	na	≤2
2	M	95	12	Age changes only	na	≤2
3	F	72	41	Age changes only	na	≤2
4	F	75	72	Age changes only	na	≤2
5	M	92	24	Age changes only	na	≤2
6	F	77	48	Age changes only	na	≤2
7	F	87	39	Age changes only	na	≤2
8	F	81	41	Age changes only	na	≤2
9	F	82	46	Age changes only	na	≤2
10	F	90	41.5	Age changes only	na	≤2
11	F	87	24	Age changes only	na	≤2
12	F	92	37	Age changes only	na	≤2
13	M	82	40	Moderate AD	75	>2 & ≤4
14	F	93	41	Mild AD	na	>2 & ≤4
15	M	89	48	Mild AD	na	>2 & ≤4
16	F	92	25	Severe CAA	84	>2 & ≤4
17	F	86	35	Mild AD	77	>2 & ≤4
18	M	91	33	Moderate AD	84	>2 & ≤4
19	F	90	6	AD	89	>2 & ≤4
20	M	86	26	AD	na	>2 & ≤4
21	F	97	25	AD	na	>2 & ≤4
22	F	84	48	AD	78	>2 & ≤4
23	M	62	50	AD	56	>4
24	M	73	36	AD	60	>4
25	F	85	24	AD	na	>4
26	F	91	45	AD	na	>4
27	F	82	46	AD	68	>4
28	F	71	64	AD	64	>4
29	F	78	70	AD	63	>4
30	F	81	25.5	AD	74	>4

PM, *post-mortem* delay; CAA, cerebral amyloid angiopathy; AD, Alzheimer's Disease; na, not applicable/available.

Table 2

Antibody sources and conditions

Antibody	Host	Dilution	Source (reference)	Secondary antibody (reference)
collagen IV	rabbit	1:500	Abcam (ab6586)	Alexa Fluor 488 (A-21202)
heparan sulphate proteoglycan (perlecan)	rat	1:500	Abcam (ab2501)	Alexa Fluor 594 (A-21209)
fibronectin	mouse	1:200	Sigma Aldrich (F0916)	Alexa Fluor 594 (A-21203)
human CD31/PECAM-1 (hPECAM)	mouse	1:100	R&D Systems (BBA7)	Alexa Fluor 594 (A-21203)
4G8	mouse	1:3000	Signet (SIG-39240)	Vectastain Elite ABC kit (PK-6100)
von Willebrand factor (vWF)	rabbit	1:200	Abcam (ab9378)	Alexa Fluor 488 (A-21202)

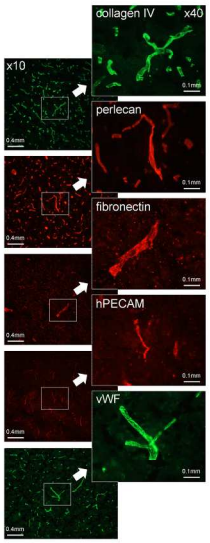

Visualisation of the different immunostaining (collagen IV, perlecan, fibronectin, hPECAM and vWF, from top to bottom) at magnification 10x (left panel, scale bars represent 0.4mm) and magnification 40x (right panel, scale bars represent 0.1mm).
209x148mm (300 x 300 DPI)

Neuropathology and Applied Neurobiology

CONFLICT OF INTEREST

Title: Early changes in extracellular matrix in Alzheimer's disease

Name: Hervé Boutin

As the corresponding author of the above manuscript which has been submitted to *Neuropathology and Applied Neurobiology,* please list below all co-authors stating whether or not they have any possible conflicts of interest. Only conflicts of interest specific to this manuscript need be declared. Please return the completed form by email or fax to the editorial office.

The following are examples of possible conflicts of interest:

1. Source of funding
2. Paid consult to sponsor
3. Study investigator funded by sponsor
4. Employee of sponsor
5. Board membership with sponsor
6. Stock holder for mentioned product
7. Patent inventor for mentioned product
8. Any financial relationship to competitors of mentioned product

This information will be kept confidential. The Editor will discuss the method of disclosure of any potential conflict of interest with authors on an individual basis.

Author	*No Conflict*	*Conflict (Please specify)*
François-Xavier Lepelletier	✗	
David M A Mann	✗	
Andrew C Robinson	✗	
Emmanuel Pinteaux	✗	
Hervé Boutin	✗	

Multiple Authorship

Please tick the box to confirm the following statement:

The corresponding author states that all authors have seen and approved the manuscript. ✓